Turbulence and Overturning Gravity Wave Effects Deduced from Mesospheric Na Density Between 100-105 Km at Andes Lidar Observatory, Chile

Channing P. Philbrick[1], Gary R. Swenson[1], Fabio A. Vargas[1], and Alan Z. Liu[2]

[1]Department of Electrical & Computer Engineering, College of Engineering, University of Illinois at Urbana-Champaign

[2]Physical Sciences Department, College of Arts & Sciences, Embry-Riddle Aeronautical University

ABSTRACT

Atmospheric turbulence activity in the mesosphere and lower thermosphere (MLT) region is determined from narrowband Na lidar measurements obtained over 27 nights between 85-105 km altitude at the Andes Lidar Observatory (ALO) in Cerro Pachón, Chile (30.3°S, 70.7°W). Photocount perturbations in the applicable spectral subrange are used as a tracer of turbulence activity. Mean altitude profiles reveal a log-scale linear increase in turbulence perturbation amplitude above 95 km. The observed trend is compared against global mean constituent transport profiles derived from SABER and SCIAMACHY satellite borne measurements.

OVERVIEW

Introduction

- Atmospheric gravity waves (AGWs) transport energy and momentum upwards to the mesosphere and lower thermosphere (MLT) region [1].
- AGWs frequently become unstable near the mesopause, breaking into turbulence and dispersing energy and momentum to the surrounding atmosphere [2].
- The atmosphere is dominated by eddy diffusion below 95 km and molecular diffusion above 105 km [3].
- Turbulent mixing in the 95-105 km transition region drives the balance between eddy and molecular diffusivity via the eddy diffusion coefficient K_{zz}, altering net constituent diffusion profiles [4].
- Minor species velocity v_s for species s is given by:

$$v_s = -D_s\left[\frac{1}{n_s}\frac{\partial n_s}{\partial z}+\frac{1}{T}\frac{\partial T}{\partial z}+\frac{m_s g}{kT}\right]-K_{zz}\left[\frac{1}{n_s}\frac{\partial n_s}{\partial z}+\frac{1}{T}\frac{\partial T}{\partial z}+\frac{mg}{kT}\right]$$

- Thorough characterization of turbulence and gravity wave dissipation in the MLT region improves middle atmospheric model accuracy.

Background

- Narrow-band, three-frequency resonance-fluorescence sodium (Na) lidar systems utilize the resident Na layer as a sensitive tracer of local wind, temperature, and density (TWD) in the 80-105 km region [5].
- K_{zz} is calculated from temperature and wind perturbation covariance and is related to the Brunt-Väisälä (BV) frequency, N^2 [6]:

$$\overline{w'T'} \approx -K_{zz}^{turb}\left(\Gamma_{ad}+\frac{\partial\overline{T}}{\partial z}\right) = -K_{zz}^{turb}N^2\frac{\overline{T}}{g}$$

- Previous efforts (e.g. [7,8]) have measured K_{zz} from 85 km to 100 km within ±10 m²/s. Above 100 km, the power-aperture product of the ALO lidar (~1 Wm²) is too weak for accurate calculation of K_{zz} [9].
- Turbulence activity can instead be measured from Na layer fluctuations following Kolmogorov's $\omega^{-5/3}$ power law at frequencies higher than N [10].
- Temperature, wind, and density fluctuations are closely related to photocount fluctuations ($N'/\overline{N}$) [9]:

$$\frac{N'}{\overline{N}} = \frac{1}{\overline{N}}\left(\frac{\partial\overline{N}}{\partial w}w'+\frac{\partial\overline{N}}{\partial T}T'+\frac{\partial\overline{N}}{\partial\rho}\rho'+\Delta N\right)$$

METHOD

Turbulence-Scale Fluctuations

1. Raw vertical count profiles (25 m, 6 s resolution) are averaged at each frequency assuming a mean temperature of $T \approx 185$ K.
2. Measurements with SNR<4 are regarded as erroneous and discarded. Remaining measurements are binned in time to 25 m, 12 s resolution.
3. Photocount profiles are normalized against the pressure scale height, $H_p(z) = kT(z)/mg$:

$$N_2(z) = N_1(z)\frac{T(z)}{T(z_0)}\exp\left\{\int_{z_0}^{z}\frac{dz}{H_p(T(z))}\right\}$$

Detrending & Filtering

4. Normalized profiles are next detrended by applying a sliding 500 m, 150 s Hamming window.
5. The detrended profiles are bandpass-filtered with cutoffs at the BV frequency and dissipative subrange (~40 mHz).

Fitting & Normalization

6. Filtered profiles are fit to an $\omega^{-5/3}$ curve at 25 m resolution. Profiles are then combined to obtain the nightly turbulence power spectral density profile.
7. Nightly neutral density turbulence power profiles (conservative) are calculated from Na fluctuations (non-conservative) by [11]:

$$\frac{n'}{\overline{n}} = \left(\frac{\gamma H_p/H_n - 1}{\gamma H_p/H_N - 1}\right)\frac{N'}{\overline{N}}$$

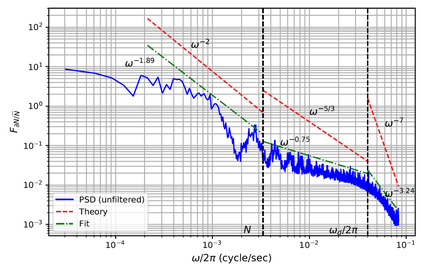

Mean temporal spectrum for the night of January 19, 2018. Average profile was calculated from 1200 independent altitude profiles with 25 m, 6 s resolution. Oblique dashed lines represent theoretical power law behavior in the applicable subrange. GW-scale variations, turbulence, and viscous dissipation respectively follow -2, -5/3, and -7 power laws. Power law fits (dash-dot) exhibit flattening in the turbulence and viscous subranges due to strong additive noise contributions. Viscous dissipation begins to dominate near 40 mHz.

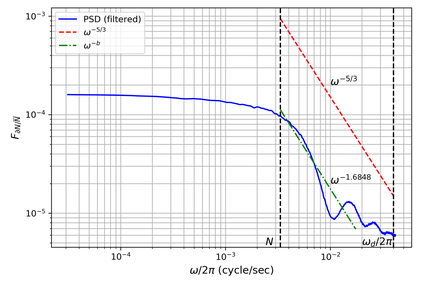

Mean temporal spectrum over 45 hours of observational ALO data. Profiles were calculated from independent altitude profiles binned to 25 m, 12 s resolution. Partial filtering of the GW subrange occurs during the detrending step, such that the ω^{-2} power law is not present. Vertical lines are cutoffs for the turbulence subrange, while the oblique dashed line represents the theoretical turbulence power law. An ω^{-b} fit to the turbulence power law (dash-dot) is also shown, where $b = -1.6848$ matches the -5/3 law within 1.1%. Additive noise begins to dominate near 20 mHz, flattening the spectral profile.

RESULTS

Data

Twenty-seven (27) nights of lidar data were acquired at ALO, spanning 2500 hours and 2375 hours of zenith and off-zenith measurements, respectively. Measurements are grouped near spring and autumnal equinoxes to leverage increased Na layer density.

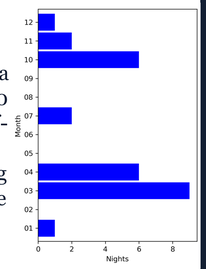

Mean Trends

- Average Na fluctuation power over the 85-105 km region is 101.7±1.67%² (10.08±0.17% amplitude).
- Na layer fluctuations are on average 5-10 times larger than neutral density fluctuations.
- Average turbulence power across the region is 6.03±1.39%² (2.46±0.57% amplitude).
- A log-scale linear increase in turbulence power is present from 95 km to 104 km, with peak power of 26.78±7.11%² (5.17±1.38% peak amplitude).

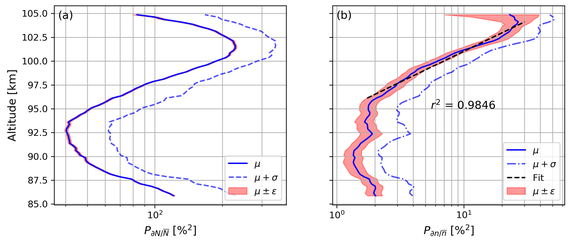

(a) Average Na turbulence fluctuation profile. Due to its dependence on the Na scale height, the measured fluctuation profile closely matches the Gaussian shape of the average sodium density profile from 87 km to 97 km.

(b) Average neutral density turbulence power profile between 85 and 105 km altitude. A log-scale linear increase in power is present from 95 km to 104 km. The solid line denotes the mean profile, the shaded region represents total uncertainty, and the dashed line shows the nightly +1σ profile variation.

SCIAMACHY & SABER Data Comparison

- Total mesospheric K_{zz} was determined from SCIAMACHY and SABER O and SABER CO_2 data [12].
- Turbulence power is related to turbulence-induced eddy diffusion by [11,13,14]:

$$K_{zz}^{turb} = \frac{\sqrt{\pi}}{4N^2}\left(\frac{P_{\partial n/\overline{n}}}{k_B^{-2/3}-k_v^{-2/3}}\right)^{3/2}$$

- The derived turbulence K_{zz} profile indicates that wave-induced turbulence plays a significant role in defining eddy transport in the 100-105 km region.

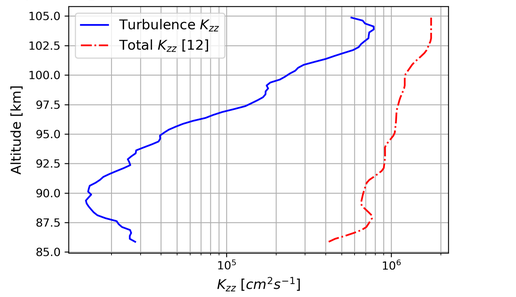

Comparison between wave-induced turbulence K_{zz} derived from Na layer fluctuations (solid) and total K_{zz} derived from global SCIAMACHY and SABER atomic oxygen and SABER CO_2 data (dot-dash). Turbulence contributes significantly to eddy diffusion above 96 km and is a significant factor in the 100-105 km region. Below 96 km, turbulence does not contribute considerably to total K_{zz}.

CONCLUSIONS

Key Findings

- Mean turbulence-induced eddy diffusion is determined from Na layer fluctuations in the 85-105 km region.
- Atmospheric sodium layer perturbations are 5-10 times more sensitive to turbulence than neutral density perturbations.
- Turbulence power exhibits a log-scale linear increase from 95-104 km with peak fluctuation amplitude of 5.17±1.38%.
- In the 100-105 km region, turbulence is a primary factor affecting total K_{zz}.

Limitations

- Mean temperature, $\overline{T}$, is the largest measurement error source. Displayed uncertainties conservatively estimate a maximum temperature error of ±10 K. At peak layer densities, an uncertainty of ±1 K is more realistic.
- Determination of turbulence K_{zz} requires averaging thousands of lidar profiles. The current power-aperture product of the ALO Na lidar does not permit intra-nightly determination of K_{zz}^{turb} in the 100-105 km region under the method described.

Future Work

- Comparison between mean K_{zz} profiles determined via the Na layer fluctuation and $\overline{w'T'}$ methods in the 85-100 km region is essential for further validation.
- Detailed explanations of the developed methodology and key findings are covered in recent [15] and forthcoming [16,17] publications.

ACKNOWLEDGMENTS

Support for C. Philbrick, G. Swenson, and F. Vargas was provided by the NSF AGS12-42895 and NSF AGS 11-10334 grants. A. Liu was supported by NSF grant AGS-1115249.

REFERENCES

[1] F. P. Bretherton, "Momentum transport by gravity waves," Quart. J. R. Met. Soc. **95**, 213-243 (1969).
[2] D. C. Fritts and T. E. Vanzandt, "Spectral estimates of gravity wave energy and momentum fluxes. Part I: Energy dissipation, acceleration, and constraints," J. Atmos. Sci **50**, 3685-3694 (1993).
[3] T. I. Gombosi, *Physics of the Space Environment*, Cam. Atmos. Space Sci. Ser., 339 pp., Cambridge University Press, Cambridge (1998).
[4] C. S. Gardner, "Role of wave-induced diffusion and energy flux in the vertical transport of atmospheric constituents in the mesopause region," J. Geophys. Res. **123**, 6581-6604 (2018).
[5] R. E. Bills, C. S. Gardner, and S. F. Franke, "Na Doppler/temperature lidar: initial mesopause region observations and comparison with the Urbana MF radar," J. Geophys. Res. **96**, 22701-22707 (1991).
[6] C. S. Gardner and W. Yang, "Measurements of the dynamical cooling rate associated with the vertical transport of heat by dissipating gravity waves in the mesopause region at the Starfire Optical Range, New Mexico," J. Geophys. Res. **103** No. D14, 16909-16926 (1998).
[7] C. S. Gardner and A. Z. Liu, "Wave-induced transport of atmospheric constituents and its effect on the mesospheric Na layer," J. Geophys. Res. **115**, D20302 (2010).
[8] Y. Guo, A. Z. Liu, and C. S. Gardner, "First Na lidar measurements of turbulence heat flux, thermal diffusivity, and energy dissipation rate in the mesopause region," Geophys. Res. Lett. **44**, 5782-5790 (2017).
[9] C. S. Gardner and A. Z. Liu, "Measuring eddy heat, constituent, and momentum fluxes with high-resolution Na and Fe Doppler lidars," J. Geophys. Res. Atmos. **119**, 10583-10603 (2014).
[10] A. Kolmogorov, "Dissipation of energy in the locally isotropic turbulence," Dokl. Akad. Nauk SSSR **32**, 16-18 (1941).
[11] E. V. Thrane and B. Grandal, "Observations of fine scale structure in the mesosphere and lower thermosphere," J. Atmos. Terr. Phys. **43** No. 3, 179-189 (1981).
[12] G. R. Swenson, University of Illinois Urbana-Champaign, private communication (2019).
[13] J. Weinstock, "Vertical turbulent diffusion in a stably stratified fluid," J. Atmos. Sci. **35**, 1022-1027 (1978).
[14] J. Weinstock, "Energy dissipation rates of turbulence in the stable free atmosphere," J. Atmos. Sci. **38**, 880-883 (1981).
[15] C. P. Philbrick, *An investigation of atmospheric turbulence in the 100-105 km region over Cerro Pachón, Chile* (Master's thesis). University of Illinois Urbana-Champaign, Urbana, Illinois (2019).
[16] C. P. Philbrick, G. R. Swenson, F. A. Vargas, and A. Z. Liu, "Sodium lidar measurements of atmospheric turbulence in the 100-105 km region," J. Atmos. Sol.-Terr. Phys., submitted May 2019.
[17] C. P. Philbrick, G. R. Swenson, F. A. Vargas, and A. Z. Liu, "Determination of mean turbulence-induced eddy diffusion from Na layer fluctuations over Cerro Pachón, Chile," Geophys. Res. Lett., submitted June 2019.

EMBRY-RIDDLE Aeronautical University DAYTONA BEACH, FLORIDA

ILLINOIS